

# Structure and Energetics of SiO<sub>2</sub> Polymorphs by Quantum-Mechanical and Semiclassical Approaches

M. Catti,\*<sup>†</sup> B. Civalleri,<sup>‡</sup> and P. Ugliengo<sup>‡</sup>

*Dipartimento di Scienza dei Materiali, Università di Milano Bicocca, via Cozzi 53, 20125 Milano, Italy, and Dipartimento di Chimica Inorganica, Fisica e dei Materiali, Università di Torino, via Giuria 5, 10125 Torino, Italy*

*Received: January 12, 2000; In Final Form: May 30, 2000*

Four SiO<sub>2</sub> polymorphs ( $\alpha$ -quartz,  $\alpha$ -cristobalite,  $\alpha$ -tridymite, and coesite) have been studied by periodic ab initio methods and by atomistic potentials. The former approach is based on all-electron localized basis sets (atomic orbitals) and on three different Hamiltonians: Hartree–Fock (HF), density functional theory in the local-density approximation (LDA), and density functional theory including gradient corrections (B3-LYP). The semiclassical approach uses interatomic potentials parametrized either on empirical observables or on ab initio theoretical properties. Full structure optimizations have been carried out, and phase transition energies derived; the results are compared with experimental data and with previous theoretical values obtained by plane-wave-pseudopotential techniques. HF and LDA structural results are slightly better than those for B3-LYP, whereas the order of performance is reversed for the relative stability of polymorphs. The quality of semiclassical data is analyzed and discussed.

## 1. Introduction

The great interest in crystalline SiO<sub>2</sub> materials and their complex polymorphism has been expressed for a long time. It is sufficient here to recall their widespread occurrence as natural phases in rocks of the earth's crust and mantle and their outstanding technological importance in catalysis, microelectronics, and optical fiber devices. In the  $p$ – $T$  phase diagram of silica, more than a dozen phases with their own stability fields can be located.<sup>1</sup> On the low-pressure end, they can be grouped into the main families of quartz, cristobalite, and tridymite, each of which contains several polymorphs. All of them have crystal structures based on frameworks of SiO<sub>4</sub> tetrahedra sharing corners. At high pressure, coesite, stishovite, and post-stishovite polymorphs are observed; in the latter two cases, SiO<sub>6</sub> coordination octahedra are present in the structures. Furthermore, there are a number of thermodynamically metastable phases (e.g., keatite and moganite). In recent years, the structural properties of most phases have been characterized satisfactorily by advanced diffraction techniques, whereas thermochemical data are still available for a minority of polymorphs only, and they are often affected by poor accuracy.

Theoretical studies of silica polymorphs by static methods (at  $T = 0$  K) have a two-fold importance. First, they aim at predicting correctly the subtle structural differences between phases, with particular emphasis on the intertetrahedral Si–O–Si angles, which show a very weak energy dependence. This is a severe test for all solid-state computational techniques, and the results are of great interest also because most structures concerned are prototypes of a great variety of frameworks in important aluminosilicate and microporous materials (zeolites, feldspars, etc.). Second, static theory can predict the relative stability of polymorphs at the athermal limit, which is usually

a good approximation of room-temperature behavior for hard materials. Such results can have a noteworthy relevance, owing to difficulties in obtaining reliable thermochemical data from experiment in many cases.

By considering periodic solid-state calculations only, both quantum-mechanical and semiclassical (atomistic potentials) techniques have been applied extensively to this problem. The state-of-the-art of the ab initio approach is summarized by two contributions, which appeared recently in the literature. The first<sup>2</sup> is based on the all-electron LCAO (linear combination of atomic orbitals) method, using Hartree–Fock and various DFT (density functional theory) Hamiltonians. Quartz and the all-silica zeolite frameworks sodalite, chabazite, faujasite, and edingtonite were studied. The main emphasis was on defining the optimal localized basis set for best results of structural and energetic properties. In the second study,<sup>3</sup> the PW-PP (plane-waves pseudopotential) method with various DFT approximations was employed, considering nine SiO<sub>2</sub> polymorphs and taking into account also the pressure dependence of the structural properties and of the relative stabilities of these phases.

The semiclassical approach is known to often provide reasonable and cheap results for the equilibrium structures, but to be intrinsically inadequate for the energetics. Temperature can be taken into account, to a first approximation, by the quasiharmonic model. A Born (Buckingham)-like two-body potential supplemented by three-body angular terms and a shell model for oxygen is generally believed to be satisfactory for aluminosilicates.<sup>4</sup> The potential parameters can be fit either to empirical crystal properties (structure, elastic constants, etc.)<sup>4,5</sup> or to ab initio derived properties of molecular clusters (bond lengths and angles and force constants).<sup>6,7</sup> Recently, the structures<sup>8</sup> and thermal expansion behavior<sup>9,10</sup> of some all-silica zeolite-like microporous frameworks and of  $\alpha$ -quartz were investigated by these methods.

In the present study, the three low-temperature  $\alpha$  phases of quartz (trigonal  $P3_221$ ), cristobalite (tetragonal  $P4_12_12$ ), and

\* Author to whom correspondence should be addressed. E-mail: catti@mater.unimib.it. Fax: +39 02 64485400.

<sup>†</sup> Università di Milano Bicocca.

<sup>‡</sup> Università di Torino

tridymite (orthorhombic  $C22_1$ ), and the high-pressure polymorph coesite (monoclinic  $C2/c$ ) are considered. We aim to investigate their structural properties and relative stabilities through a combined approach based on the ab initio periodic LCAO scheme and various model potential calculations. The first objective is to compare periodic quantum-mechanical results based on different Hamiltonians with one another and to compare the use of all-electron localized basis sets (this work) with that of pseudopotential-plane-wave techniques (literature data). As a second objective, we assess the reliability of the cheaper semiclassical simulations by comparison with first-principles methods and the feasibility of mixed approaches. Indeed, the idea of combining cheap structure optimizations based on model potentials with ab initio total energy calculations is attractive and deserves to be tested for subsequent applications to complex aluminosilicate systems.

## 2. Computational Methods

**2.1. Ab Initio Calculations.** All quantum-mechanical calculations were carried out by the computer code CRYSTAL98,<sup>11</sup> implementing a periodic LCAO approach in which the SCF (self-consistent-field) equations for one-electron eigenvalues and crystalline orbitals can be solved by use of a variety of Hamiltonians. In the present study, three are employed: Hartree–Fock, DFT-LDA (local-density approximation), and DFT-B3-LYP. They will be indicated below by the abbreviations HF, LDA, and B3, respectively. In the HF scheme, the exchange interaction between electrons is represented exactly by a nonlocal functional, while the electron correlation is neglected completely. However, we have supplemented the HF total energy by an a posteriori DFT-GGA (generalized gradient approximation) estimate of the correlation contribution based on the Hartree–Fock electron density,<sup>12</sup> which will be given separately in the results below. The LDA Hamiltonian is based on approximate local functionals for both the exchange and the correlation effects. The S-VWN parametrization was used, according to Slater’s exchange<sup>13</sup> and Vosko–Wilk–Nusair’s correlation<sup>14</sup> potentials. Eventually, the B3-LYP case is a combination of Becke’s<sup>15</sup> and Hartree–Fock potentials for the exchange effect and uses the gradient-corrected correlation functional of Lee–Yang–Parr.<sup>16</sup>

All-electron localized basis sets were used to represent the atomic orbitals of Si and O. The radial factors are expressed as linear combinations of Gaussian-type functions of the electron-nucleus distance, according to standard Pople’s 6-6-21G(d) scheme for silicon [with the outermost exponents  $\alpha(\text{sp}) = 0.13$  and  $\alpha(\text{d}) = 0.5 \text{ b}^{-2}$ ] and to the 6-31G(d) scheme for oxygen [with the outermost exponents  $\alpha(\text{sp}) = 0.27$  and  $\alpha(\text{d}) = 0.6 \text{ b}^{-2}$ ]. This basis set was optimized and proved to be fully adequate for  $\text{SiO}_2$  systems in a previous study.<sup>2</sup> Upon employing DFT Hamiltonians, the exchange-correlation potential is expanded in an auxiliary basis set of Gaussian-type functions.<sup>17</sup> At each SCF cycle, the expansion coefficients are fit to the actual analytic form of the exchange-correlation potential, which changes with the evolving charge density.

The level of numerical approximation in evaluating the Coulomb and exchange series appearing in the SCF equations for periodic systems is controlled by five tolerances.<sup>11</sup> These are related to estimates of overlap or penetration for integrals of Gaussian functions on different centers, which define cutoff limits for series summation. The values used in the present calculations are  $10^{-6}$ ,  $10^{-6}$ ,  $10^{-6}$ ,  $10^{-6}$ , and  $10^{-12}$ . The reciprocal space was sampled according to a regular sublattice defined by six to eight points in the irreducible Brillouin zone.

The structure optimizations were performed by the LoptCG routine written by C. Zicovich-Wilson, which is based on computation of numerical derivatives of the total energy with respect to structural variables (central-difference formula) and subsequent processing by conjugate gradients (modified Polak–Ribière algorithm).<sup>2</sup> Lattice constants and atomic fractional coordinates were optimized at the same time, and convergence was considered to be attained when the square root of the mean weighted gradient norm was less than  $0.01 \text{ hartree}^{1/2}$ .

**2.2. Atomistic Potentials.** The computer code GULP<sup>18</sup> was used for calculations based on model interatomic potentials. Three types of ionic potentials for Si–O systems were taken from the literature. The first two,<sup>6,7</sup> particularly intended for application to open-structure microporous phases, share the same analytical form: a shell model for the  $\text{O}^{2-}$  ion (the core and shell charges add up to  $-2 \text{ e}$ ; the core and shell interact by a harmonic spring constant), a two-body electrostatic interaction for all ion pairs, an exponential repulsion for the Si–O pair, and a three-body harmonic interaction for the O–Si–O bond angle. In both cases, the potential parameters were fit to ab initio computed structural features and vibrational frequencies of a variety of molecular clusters, with geometries simulating fragments of microporous zeolite-like systems. The difference lies in the ab initio technique used to derive the theoretical properties: by parametrization on Hartree–Fock or DFT-B3LYP results, respectively, the G(HF)<sup>6</sup> and G(B3)<sup>7</sup> potentials are obtained. The third potential,<sup>5</sup> on the other hand, is parametrized on empirical properties (structure and elastic constants) of  $\alpha$ -quartz, and will be denoted as G(JC). Its analytical form differs slightly from the previous one, because of the additional presence of the O–O exponential repulsion.

The GULP code was used not only to perform structural optimizations of the different  $\text{SiO}_2$  polymorphs, but also to compute their zero-point vibrational energies, which may be important in determining the crystal cohesion energies at  $T = 0 \text{ K}$ . This is made possible by a full lattice-dynamical calculation of the vibrational frequency spectrum of each crystal, within the frame of the harmonic approximation.

## 3. Results

**3.1. Structural Properties.** For each of the three polymorphs,  $\alpha$ -quartz,  $\alpha$ -cristobalite, and  $\alpha$ -tridymite, the least-energy crystal structure (unit-cell edges and atomic fractional coordinates unconstrained by symmetry) was searched for by six separate calculations (HF, B3, and LDA: ab initio approach with the corresponding Hamiltonians; G(HF), G(B3), and G(JC): semiclassical approach with the corresponding model potentials). The results are reported in Tables 1–3 and compared to experimental structural data and to the most recent PW-PP-LDA theoretical values. Several accurate room-temperature diffraction studies of the concerned  $\text{SiO}_2$  phases are present in the literature.<sup>19–26</sup> However, where available ( $\alpha$ -quartz<sup>22</sup> and  $\alpha$ -cristobalite<sup>24</sup>), we have selected for comparison low-temperature results, because even small thermal expansion effects may be important for an accurate evaluation of theoretical data.

In the case of  $\alpha$ -tridymite, the eight atomic fractional coordinates unconstrained by symmetry (for Si,  $x, y, z$ ; for O1,  $x, 0, 0$ ; for O2,  $0, y, 3/4$ ; and for O3,  $x, y, z$ ) have not been reported in Table 3 for brevity. The total energy values appearing in the columns of atomistic potentials of each table actually refer to ab initio calculations performed by the HF, B3, and HF Hamiltonians for the structures optimized by the G(HF), G(B3), and G(JC) potentials, respectively. HF energies corrected a posteriori for correlation effects are given in parentheses.

**TABLE 1: Unit-cell Constants, Volume Per Formula Unit, Fractional Atomic Coordinates, Average Si–O Bond Length, Si–O–Si Bond Angle, and Total Energy Per Formula Unit for the Simulated Structures of  $\alpha$ -Quartz ( $P3_121$ ,  $Z = 3$ ), Compared to Experimental Data<sup>22</sup> and to Plane-Wave LDA Literature Values<sup>3a</sup>**

	expt <sup>22</sup>			ab initio						atomistic potentials		
	296 K	13 K		HF	B3	LDA	PW-LDA <sup>3</sup>	G(HF)	G(B3)	G(JC)		
$a$ (Å)	4.914	4.902	4.953	4.915	4.955	4.917	4.840	4.870	4.899	4.988	4.890	4.837
			1.0%	0.3%	1.1%	0.3%	−1.3%	−0.7%	−0.1%	1.8%	−0.2%	−1.3%
$c$ (Å)	5.406	5.400	5.427	5.406	5.428	5.434	5.394	5.386	5.383	5.506	5.452	5.347
			0.5%	0.1%	0.5%	0.6%	−0.1%	−0.3%	−0.3%	2.0%	1.0%	−1.0%
$V$ (Å <sup>3</sup> )	37.7	37.5	38.4	37.7	38.5	37.9	36.5	36.9	37.3	39.5	37.6	36.1
			2.4%	0.5%	2.7%	1.1%	−2.7%	−1.6%	−0.5%	5.3%	0.3%	−3.7%
$x$ (Si)	0.4700	0.4680	0.4714	0.4656	0.4647	0.4621	0.4628	0.4618	0.4695	0.4740	0.4607	0.4639
$x$ (O)	0.4131	0.4124	0.4153	0.4145	0.4131	0.4114	0.4049	0.4082	0.4143	0.4222	0.4127	0.4083
$y$ (O)	0.2677	0.2712	0.2652	0.2746	0.2773	0.2807	0.2808	0.2830	0.2670	0.2628	0.2867	0.2784
$z$ (O)	0.1189	0.1163	0.1213	0.1149	0.1112	0.1092	0.1065	0.1056	0.1199	0.1260	0.1051	0.1087
$\langle\text{Si–O}\rangle$ (Å)	1.610	1.613	1.614	1.617	1.636	1.635	1.626	1.630	1.605	1.616	1.639	1.612
$\angle\text{Si–O–Si}$ (°)	143.5	142.4	144.8	142.4	141.0	139.8	137.5	137.9	144.1	147.8	138.5	139.1
$E$ (hartree)			−438.8865	−438.8863	−440.0385	−440.0384	−437.9564	−437.9563		−438.8861	−440.0381	−438.8855
			(−440.0848)	(−440.0848)								

<sup>a</sup> Optimized structures refer to Hartree–Fock, DFT-B3LYP, and DFT-LDA Hamiltonians (two distinct energy minima are reported in each case) and to three semiclassical atom–atom potentials (see the text). HF energy values, including the a posteriori correction for correlation, are given in parentheses. Relative deviations of theoretical lattice constants are referred to experimental values at 13 K.

**TABLE 2: Results for Structural Data of  $\alpha$ -Cristobalite ( $P4_12_12$ ,  $Z = 4$ ), Compared to Experimental Data<sup>24</sup> and to Plane-Wave LDA Literature Values<sup>3a</sup>**

	expt <sup>24</sup>		ab initio				atomistic potentials		
	298 K	10 K	HF	B3	LDA	PW-LDA <sup>3</sup>	G(HF)	G(B3)	G(JC)
$a$ (Å)	4.971	4.957	4.968	4.989	4.959	4.975	5.129	4.981	4.972
			0.2%	0.6%	0.0%	0.4%	3.5%	0.5%	0.3%
$c$ (Å)	6.928	6.890	6.893	6.902	6.918	6.926	7.267	7.167	7.010
			0.0%	0.2%	0.4%	0.5%	5.5%	4.0%	1.7%
$V$ (Å <sup>3</sup> )	42.8	42.3	42.5	42.9	42.5	42.9	47.8	44.5	43.3
			0.5%	1.4%	0.5%	1.4%	13.0%	5.2%	2.4%
$x$ (Si)	0.3005	0.3047	0.3049	0.3069	0.3043	0.2988	0.2798	0.2999	0.2939
$x$ (O)	0.2392	0.2381	0.2370	0.2362	0.2361	0.2399	0.2457	0.2379	0.2405
$y$ (O)	0.1037	0.1109	0.1134	0.1188	0.1172	0.1007	0.0639	0.1095	0.0969
$z$ (O)	0.1786	0.1826	0.1827	0.1866	0.1859	0.1768	0.1585	0.1801	0.1767
$\langle\text{Si–O}\rangle$ (Å)	1.603	1.609	1.614	1.631	1.624	1.598	1.607	1.630	1.601
$\angle\text{Si–O–Si}$ (°)	146.7	144.7	144.2	142.1	142.0	147.7	158.5	145.2	147.3
$E$ (hartree)			−438.8863	−440.0380	−437.9529		−438.8859	−440.0378	−438.8859
			(−440.0840)						

<sup>a</sup> Relative deviations of theoretical lattice constants are referred to experimental values at 10 K.

**TABLE 3: Results for Structural Data of  $\alpha$ -Tridymite ( $C222_1$ ,  $Z = 8$ ), Compared to Room-Temperature Experimental Data<sup>26</sup> and to Plane-Wave LDA Literature Values<sup>3a</sup>**

	expt <sup>26</sup>	ab initio				atomistic potentials		
		HF	B3	LDA	PW-LDA <sup>3</sup>	G(HF)	G(B3)	G(JC)
$a$ (Å)	8.756	9.031	9.102	9.061	8.977	9.063	9.145	8.666
		3.1%	3.9%	3.5%	2.5%	3.5%	4.4%	−1.0%
$b$ (Å)	5.024	5.057	4.994	4.962	5.008	5.152	5.050	4.993
		0.7%	−0.6%	−1.2%	−0.3%	2.5%	0.5%	−0.6%
$c$ (Å)	8.213	8.220	8.143	8.104	8.179	8.405	8.255	8.337
		0.1%	−0.9%	−1.3%	−0.4%	2.3%	0.5%	1.5%
$V$ (Å <sup>3</sup> )	45.2	46.9	46.3	45.5	46.0	49.1	47.7	45.1
		3.8%	2.4%	0.7%	1.8%	8.6%	5.5%	−0.2%
$\langle\text{Si–O}\rangle$ (Å)	1.559	1.606	1.612	1.613	1.590	1.603	1.623	1.595
$\angle\text{Si–O–Si}$ (°)	179.7	178.9	176.8	175.0	178.2	178.9	176.3	176.2
	171.0	169.2	169.5	172.3	175.1	174.8	172.6	144.7
	160.6	150.0	142.6	141.4	150.4	160.1	146.3	148.4
$E$ (hartree)		−438.8856	−440.0368	−437.9514		−438.8853	−440.0368	−438.8856
		(−440.0834)						

<sup>a</sup> The eight free atomic fractional coordinates are not reported for brevity.

For all three polymorphs and each computational method, the structure optimization was carried out starting from the experimental unit cell and atomic coordinates as initial values. However, we tried also to use the semiclassically optimized structures as initial guesses for the quantum-mechanical energy minimizations. In the cases of  $\alpha$ -cristobalite and  $\alpha$ -tridymite, a unique energy minimum was found (Tables 2 and 3), whereas

for  $\alpha$ -quartz, two distinct minima with very close energy values were obtained, according to the different starting points (Table 1). This surprising result is not accidental, because it is observed by use of any of the three Hamiltonians HF, B3, and LDA, and is actually related to the peculiar flatness of the  $\alpha$ -quartz potential energy surface in the region around the two minima. Indeed, the energy differences of the pairs of optimized  $\alpha$ -quartz

**TABLE 4: Results for Structural Data of Coesite (C2/c,  $Z = 16$ ), Compared to Room-Temperature Experimental Data<sup>27</sup>**

	expt <sup>27</sup>	G(HF)	G(B3)	G(JC)
<i>a</i> (Å)	7.136	7.187 0.7%	7.179 0.6%	7.027 −1.5%
<i>b</i> (Å)	12.369	12.538 1.4%	12.595 1.8%	12.291 −0.6%
<i>c</i> (Å)	7.174	7.256 1.1%	7.254 1.1%	7.115 −0.8%
$\beta$ (°)	120.3	122.8 2.1%	123.8 2.9%	122.5 1.8%
<i>V</i> (Å <sup>3</sup> )	34.2	34.4 0.6%	34.1 −0.3%	32.4 −5.3%
$\langle\text{Si}-\text{O}\rangle$ (Å)	1.611	1.620	1.639	1.607
$\angle\text{Si}-\text{O}-\text{Si}$ (°)	180	180	180	180
	142.7	142.9	137.8	136.4
	144.5	141.1	135.6	136.7
	149.7	151.1	147.6	147.6
	137.3	138.0	133.0	132.6
<i>E</i> (hartree)		−438.8824	−440.0338	−438.8802

**TABLE 5: Theoretical Energies (kJ mol<sup>−1</sup>) of SiO<sub>2</sub> Polymorphs Referred to the Energy of  $\alpha$ -Quartz at  $T = 0$  K, Including the Zero-Point Vibrational Contributions<sup>a</sup>**

	$\alpha$ -cristobalite	$\alpha$ -tridymite	coesite
HF	0.0	1.5	
HF+corr.	2.2	3.5	
B3	1.4	4.0	
LDA	9.3	12.6	
HF//G(HF)	0.5	1.8	9.7
B3//G(B3)	0.9	3.3	10.9
HF//G(JC)	−1.1	−0.5	13.6
B3//G(JC)	2.4	3.7	11.1
G(HF)	−3.8	−3.0	6.8
G(B3)	1.6	7.4	7.2
G(JC)	3.5	4.9	1.8
expt <sup>28</sup>	2.8 ± 2.2	3.2 ± 2.6	5.1 ± 2.3
expt <sup>29</sup>	2.6	2.9	3.8

<sup>a</sup> Experimental values are reported for comparison.

structures are hardly significant ( $1-2 \times 10^{-4}$  hartree), and they are roughly comparable with the largest  $\Delta E$  variations in the whole region. Unfortunately, tightening the convergence criteria would scarcely help to find the “true” single minimum, because of intrinsic limits on the numerical accuracy of the computational method used.

In the case of monoclinic coesite, which has 20 structural degrees of freedom, we did not optimize the structure by any of the quantum-mechanical methods for reasons of computational cost. Energy minimizations were thus carried out by the atomistic potentials only, and then ab initio energies were computed for the corresponding semiclassically optimized structures. The results are reported in Table 4 and compared to room-temperature experimental data.<sup>27</sup>

**3.2. Relative Stability.** An important piece of information coming out of total energy calculations in a family of polymorphs concerns the energetics of phase transitions at 0 K. Here,  $\alpha$ -quartz has been taken as the reference phase, and energy differences of  $\alpha$ -cristobalite,  $\alpha$ -tridymite and coesite with respect to this reference have been reported in Table 5. The first four lines contain full ab initio results, the following four lines refer to ab initio energies computed for semiclassically optimized structures, and the subsequent three lines report full semiclassical results.

Two sets of experimental data are provided for comparison. The first<sup>28</sup> comes from calorimetric measurements, which are the most direct experimental technique but which are also affected by considerable uncertainty. The second set of data<sup>29</sup> also takes into account information from phase diagrams, but

no estimated errors are provided. All of these experimental results refer to 298 K, and the temperature effect should be estimated for comparison with theoretical static data at 0 K. It is known that the zero-point vibrational energy is often not negligible<sup>30</sup> and gives, by far, the largest contribution to the energy difference of an ionic solid between room temperature and the static athermal limit. Thus,  $E_{\text{vib}}^0$  was computed by GULP for each of the four phases, using the G(HF) and G(B3) interatomic potentials; the values  $\Delta E_{\text{vib}}^0[\text{G(HF)}] = 0.0, -0.2, -0.2 \text{ kJ mol}^{-1}$  and  $\Delta E_{\text{vib}}^0[\text{G(B3)}] = 0.2, -0.3, -0.3 \text{ kJ mol}^{-1}$  were obtained for the relative vibrational energies of cristobalite, tridymite, and coesite, respectively, with respect to quartz and were included in the total energy differences reported in Table 5.

## 4. Discussion

**4.1. Ab Initio Simulations.** The result obtained for the  $\alpha$ -quartz structure, that very close but distinct ab initio energy minima may ensue from different optimization starting points, proves this energy hypersurface to be very flat with respect to the state-of-the-art attainable numerical accuracy.<sup>31</sup> In particular, as in each case the two least-energy structures (Table 1) differ mainly by the *a* cell edge and Si—O—Si angle, there seems to be a high correlation between these structural parameters in the  $\alpha$ -quartz structure. In a limited range, the unit cell may be expanded along *a* with no significant change in the Si—O distance, just by flattening the Si—O—Si angle, at a vanishing energy cost. This outcome of our calculations is consistent with the findings of a theoretical study on the disiloxane molecule ( $\text{H}_3\text{SiOSiH}_3$ ).<sup>32</sup> Experimental evidence gives a bent equilibrium Si—O—Si angle of 150°, with an energy barrier to molecular linearization of only  $5 \times 10^{-4}$  hartree. To reproduce these results theoretically, it was necessary to use a very extended basis set, including electron correlation at the MP2 (Moeller–Plesset 2) level. As solid-state computational techniques cannot presently afford this level of sophistication, there may be intrinsic limits for resolving the small energy differences that separate different configurations of tectosilicate phases in the neighborhood of the absolute minimum.

Despite this problem, on the average, the theoretical lattice constants of  $\alpha$ -quartz lie within 1% of the experimental values, when the less favorable of the two energy minima is also considered. Even smaller errors are observed for  $\alpha$ -cristobalite (Table 2), whereas in the case of  $\alpha$ -tridymite (Table 3), the results are not as satisfactory for the *a* cell edge and the Si—O bond length. In this case, the computed values are systematically overestimated by over 3%, including the LDA results, which usually tend to shorten lattice constants and interatomic distances. Such results are also consistent with the previous PW-LDA study<sup>3</sup> and seem to indicate that the suggested disorder<sup>26</sup> in the observed structure at 493 K is probably responsible for deviations from all static theoretical results obtained so far.

Within a roughly comparable quality for the performances of the three Hamiltonians used, the best score can be given to Hartree–Fock, followed closely by LDA, and then by B3-LYP. The latter method gives slightly larger unit-cell edges and Si—O bond lengths; this is consistent with the general observation that gradient-corrected functionals systematically overestimate the interatomic distances.<sup>3</sup> In the case of Si—O—Si angles, again HF results are slightly better than those of B3-LYP and LDA, but the LDA value for  $\alpha$ -quartz appears to be significantly underestimated. As for  $\alpha$ -tridymite, the smallest of its three independent Si—O—Si angles is predicted by all Hamiltonians to be more bent than the experimental value, also confirming



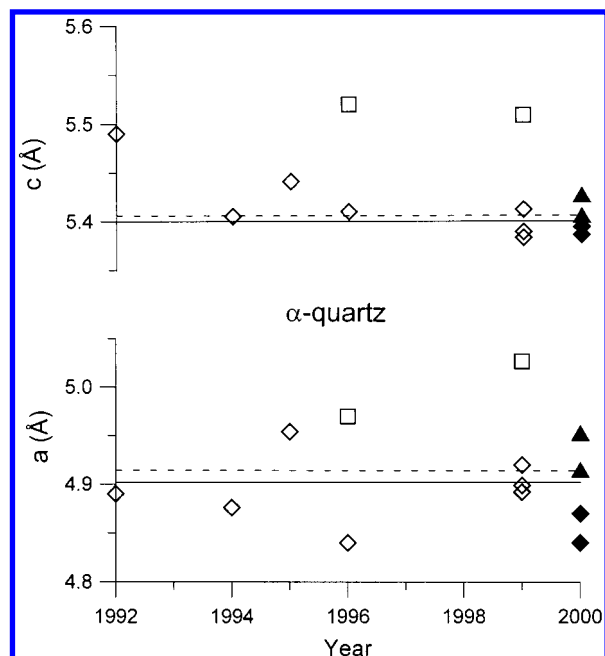


**Figure 1.** Ab initio optimized lattice constants of  $\alpha$ -quartz from literature of the past decade<sup>3,33–38</sup> (PW-PP-DFT, open symbols) and from this work (all-electron LCAO, closed symbols), compared to experimental values<sup>22</sup> at 13 K (full lines) and 296 K (dashed lines). Diamonds, squares, and triangles correspond to LDA, GGA, and Hartree-Fock Hamiltonians, respectively.

previous results.<sup>3</sup> This is probably related to the need for accommodating longer Si–O bonds with respect to the observed values in the theoretical structure.

It is interesting to compare our results, obtained by all-electron localized basis functions, with previous calculations performed by plane-wave-pseudopotential basis sets (LDA and GGA functionals). The most recent PW-PP-LDA results<sup>3</sup> for all three SiO<sub>2</sub> polymorphs considered have been included in Tables 1–3. Furthermore, literature data from the past decade for  $\alpha$ -quartz<sup>3,33–38</sup> and  $\alpha$ -cristobalite<sup>3,34</sup> have been plotted versus publication year in Figures 1 and 2 (unit-cell constants) and Figures 3 and 4 (Si–O–Si angle), together with our results using the HF and LDA functionals and with experimental data at low and room temperature.<sup>22,24</sup> An important feature affecting the different PW-PP calculations and their performance is the way pseudopotentials are generated. We can distinguish between norm-conserving and ultra-soft pseudopotentials; the former require a larger PW basis set and energy cutoff than the latter for an accurate description of the valence electrons. Norm-conserving PPs generated according to Teter,<sup>35</sup> Troullier-Martins,<sup>33,37</sup> and Hamann<sup>36</sup> and ultra-soft PPs according to Vanderbilt<sup>3,34,38</sup> have been used.

By inspection of Figures 1–4, the following conclusions can be derived. (i) PW-PP-GGA results largely overestimate both the lattice constants and the Si–O–Si angle and are thus of much poorer quality than all others. (ii) Within PW-PP-LDA data, those obtained by ultra-soft pseudopotentials perform best. (iii) Our HF results are excellent and similar to the best PW-PP-LDA data,<sup>3</sup> if the most favorable of the two energy minima of  $\alpha$ -quartz is considered; by taking the other minimum into account, the results are still within the spread of PW-PP-LDA values. (iv) Our LCAO-LDA data are fully satisfactory, but for  $\alpha$ -quartz, they show slightly smaller values of the *a* cell edge and of the Si–O–Si angle with respect to the best PW-PP-LDA results.<sup>3</sup> The larger bending of the intertetrahedral angle should ensue directly from the stronger lattice contraction.

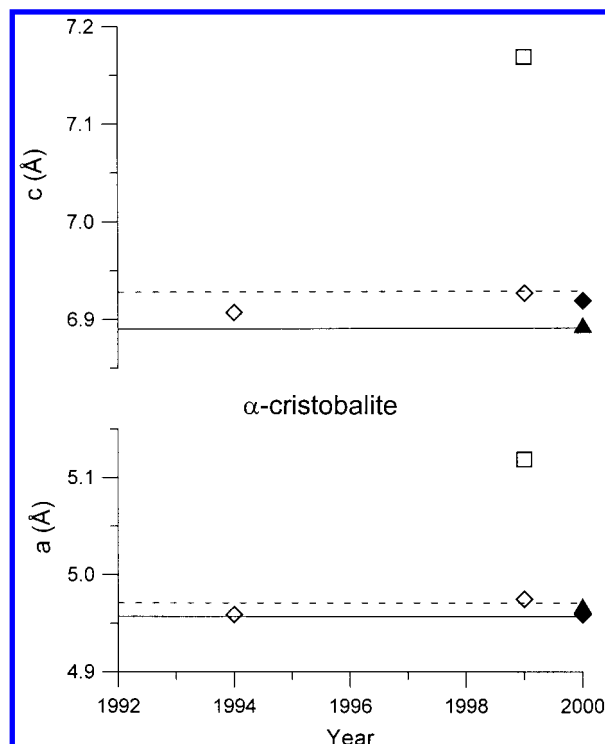


**Figure 2.** Ab initio optimized lattice constants of  $\alpha$ -cristobalite from literature of the past decade<sup>3,34</sup> (PW-PP-DFT, open symbols) and from this work (all-electron LCAO, closed symbols), compared to experimental values<sup>24</sup> at 10 K (full lines) and 298 K (dashed lines). Diamonds, squares, and triangles correspond to LDA, GGA, and Hartree-Fock Hamiltonians, respectively.

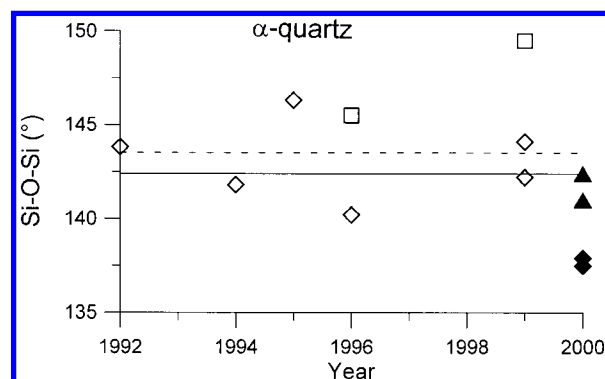


**Figure 3.** Ab initio optimized Si–O–Si angle of  $\alpha$ -quartz (cf. Figure 1 for explanations).

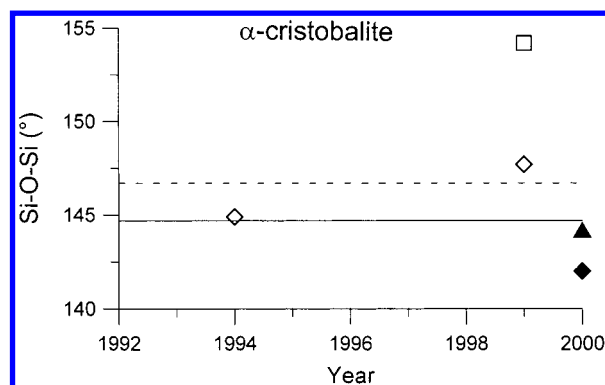


**Figure 4.** Ab initio optimized Si–O–Si angle of  $\alpha$ -cristobalite (cf. Figure 2 for explanations).

As for the ab initio energetics of  $\alpha$ -cristobalite and  $\alpha$ -tridymite versus  $\alpha$ -quartz (Table 5), the order of stability is predicted correctly in all cases, with the doubtful case of HF results which

show quartz and cristobalite to be equally stable. The quantitative agreement with experiment is best for the HF data corrected a posteriori for correlation (with a GGA functional), followed by the B3-LYP results; both sets of data give energies within the reported uncertainty of the experimental values.<sup>28</sup> Uncorrected HF and LDA results underestimate and overestimate, respectively, the energy of  $\alpha$ -quartz with respect to the those of the other two polymorphs. Our result is at variance with that obtained by the PW-PP method,<sup>3</sup> for which LDA energies show a much better agreement with experiment than the GGA results, but is consistent with knowledge from molecular calculations. In that case, indeed, use of the generalized-gradient approximation is known to improve the quality of binding energies significantly with respect to the local-density functional.

**4.2. Atomistic Potentials.** By examining the structural results obtained by semiclassical methods (Tables 1–4), the empirical potential JC appears to perform better, on the whole, than both first-principles potentials G(HF) and G(B3). This is not an obvious result, because the relative performance of JC is better for the polymorphs other than  $\alpha$ -quartz (cf, in particular, the tridymite case), while its potential parameters were fit to just the  $\alpha$ -quartz observables. We are thus more inclined to ascribe the result to an insufficiency of the G(HF) and G(B3) potentials, rather than to a particular success of the empirical potential. This is also confirmed by considering the much larger deviations from experiment of the G(HF) and G(B3) results with respect to the corresponding ab initio HF and B3 data. The comparatively modest performance of the first-principles potentials is probably related to their lacking of O–O repulsion terms. These terms may possibly be neglected for applications to low-density microporous zeolite-like phases, but should be quite important in accounting for structural features of denser SiO<sub>2</sub> polymorphs. Any future effort at improving the quality of such potentials should, therefore, take this problem into account. By comparing the G(HF) and G(B3) results to each other, the latter appear to be definitely better, except for a tendency to give Si–O bond distances that are too long. The case of the most complicated structure, coesite, differs somehow from that of the other polymorphs, because in this case, all three atomistic potentials give quite satisfactory agreements with the experiment (Table 4).

With reference to the relative stability of SiO<sub>2</sub> polymorphs (Table 5), good results are obtained with the mixed procedure of computing ab initio energies for structures optimized semiclassically with consistent ab initio parametrized potentials [HF//G(HF) and B3//G(B3) cases]. The relative energies obtained are similar to full ab initio results, at least for the  $\alpha$ -cristobalite and  $\alpha$ -tridymite polymorphs. As for the full semiclassical values, a wrong order of stability is observed for G(HF), whereas the results are qualitatively correct in the G(B3) case.

## 5. Conclusions

Periodic ab initio Hartree–Fock and DFT-LDA calculations, with all-electron atomic orbital basis sets, have been shown to predict the structural properties of several SiO<sub>2</sub> polymorphs very satisfactorily, with errors below 1% on the average for the unit-cell edges (the peculiar case of tridymite was discussed in detail above). This is comparable to the state-of-the-art PW-PP data. However, results obtained for  $\alpha$ -quartz show that, for best accuracy, the structure optimization should be checked very carefully in the neighborhood of the energy minimum, because there the energy hypersurface is very flat. Gradient corrections to the exchange-correlation functional (B3-LYP Hamiltonian) give slightly less satisfactory results for the structure, but

improve significantly the predicted energetics of phase transitions; in this respect, a posteriori application of the GGA correction for correlation to the HF density also performs very well. In the case of atomistic potentials, it should be possible to improve the performance of those parametrized on ab initio data by revising their analytical form, so as to take account of O–O repulsion. A combined use of quantum-mechanical and semiclassical methods may be very useful for predicting the relative stability of phases with very complex crystal structures at a low computational cost.

**Acknowledgment.** The present work is part of the research projects cofinanced by the Italian MURST and coordinated by A. Zecchina (Cofin98, Area 03) and by C. Giacobbo (Cofin99, Area 04). We thank Roberto Dovesi for useful discussions and for his interest in this work.

## References and Notes

- (1) Heany, P. J.; Prewitt, C. T.; Gibbs, G. V., Eds. *Silica. Physical Behaviour, Geochemistry and Materials Applications*; Mineralogical Society of America: Washington, D.C., 1994.
- (2) Civalleri, B.; Zicovich-Wilson, C. M.; Ugliengo, P.; Saunders, V. R.; Dovesi, R. *Chem. Phys. Lett.* **1998**, *292*, 394.
- (3) Demuth, Th.; Jeanvoine, Y.; Hafner, J.; Ángyán, J. G. *J. Phys.: Condens. Matter* **1999**, *11*, 3833.
- (4) Sanders, M. J.; Leslie, M.; Catlow, C. R. A. *J. Chem. Soc., Chem. Commun.* **1984**, 1271.
- (5) Jackson, R. A.; Catlow, C. R. A. *Mol. Simul.* **1988**, *1*, 207.
- (6) Schröder, K. P.; Sauer, J. *J. Phys. Chem.* **1996**, *100*, 11043.
- (7) Sierka, M.; Sauer, J. *Faraday Discuss.* **1997**, *106*, 41.
- (8) De Boer, K.; Jansen, A. P. J.; van Santen, R. A. *Phys. Rev. B* **1995**, *52*, 12579.
- (9) Tschafeser, P.; Parker, S. C. *J. Phys. Chem.* **1995**, *99*, 10609.
- (10) Gale, J. D. *J. Phys. Chem. B* **1998**, *102*, 5423.
- (11) Saunders, V. R.; Dovesi, R.; Roetti, C.; Causà, M.; Harrison, N. M.; Orlando, R.; Zicovich-Wilson, C. M. *CRYSTAL98*; University of Torino, Torino, Italy, and CLRC Daresbury Laboratory, Warrington, Cheshire, U.K., 1999.
- (12) Perdew, J. P.; Chevary, J. A.; Vosko, S. H.; Jackson, K. A.; Pederson, M. R.; Singh, D. J.; Fiolhais, C. *Phys. Rev. B* **1992**, *46*, 6671.
- (13) Slater, J. C. *The Self-Consistent Field for Molecules and Solids; Quantum Theory of Molecules and Solids*, Vol. 4; McGraw-Hill: New York, 1974.
- (14) Vosko, S. H.; Wilk, L.; Nusair, M. *Can. J. Phys.* **1980**, *58*, 1200.
- (15) Becke, A. D. *Phys. Rev. A* **1988**, *38*, 3098.
- (16) Lee, C.; Yang, W.; Parr, R. G. *Phys. Rev. B* **1988**, *37*, 785.
- (17) Towler, M. D.; Zupan, A.; Causà, M. *Comput. Phys. Comm.* **1996**, *98*, 181.
- (18) Gale, J. D. *GULP (General Utility Lattice Program)*; Royal Institution/Imperial College: London, U.K., 1992–1994.
- (19) Levien, L.; Prewitt, C. T.; Weidner, D. J. *Am. Mineral.* **1980**, *65*, 920.
- (20) Will, G.; Bellotto, M.; Parrish, W.; Hart, M. *J. Appl. Crystallogr.* **1988**, *21*, 182.
- (21) Wright, A. F.; Lehmann, M. S. *J. Solid State Chem.* **1981**, *36*, 371.
- (22) Lager, G. A.; Jorgensen, J. D.; Rotella, F. J. *J. Appl. Phys.* **1982**, *53*, 6751.
- (23) Schmahl, W. W.; Swainson, I. P.; Dove, M. T.; Graeme-Barber, A. *Z. Kristallogr.* **1992**, *201*, 125.
- (24) Pluth, J. J.; Smith, J. V.; Faber, J. *J. Appl. Phys.* **1985**, *57*, 1045.
- (25) Kihara, K. *Z. Kristallogr.* **1978**, *148*, 237.
- (26) Kihara, K.; Matsumoto, T.; Imamura, M. *Z. Kristallogr.* **1986**, *177*, 27.
- (27) Levien, L.; Prewitt, C. T. *Am. Mineral.* **1981**, *66*, 324.
- (28) Petrovic, I.; Heaney, P. J.; Navrotsky, A. *Phys. Chem. Minerals* **1996**, *23*, 119.
- (29) Saxena, S. K.; Chatterjee, N.; Fei, Y.; Shen, G. *Thermodynamic Data on Oxides and Silicates*; Springer-Verlag: Berlin, 1993.
- (30) Catti, M.; Valerio, G.; Dovesi, R.; Causà, M. *Phys. Rev. B* **1994**, *49*, 14179.
- (31) Supplementary calculations run by one of us with the CASTEP code (Payne, M. C.; Teter, M. P.; Allan, D. C.; Arias, T. A.; Joannopoulos, J. D. *Rev. Mod. Phys.* **1992**, *64*, 1045) using a GGA/pseudopotential plane-wave approach with analytical gradients confirmed the difficulty of finding a single well-defined energy minimum for  $\alpha$ -quartz.
- (32) Bär, M. R.; Sauer, J. *Chem. Phys. Lett.* **1994**, *226*, 405.
- (33) Keskar, N. R.; Chelikowsky, J. R. *Phys. Rev. B* **1992**, *46*, 1.

- (34) Liu, F.; Garofalini, S. H.; King-Smith, D.; Vanderbilt, D. *Phys. Rev. B* **1994**, 49, 12528.
- (35) Teter, D. M.; Gibbs, G. V.; Boisen, M. B., Jr.; Allan, D. C.; Teter, M. P. *Phys. Rev. B* **1995**, 52, 8064.

- (36) Hamann, D. R. *Phys. Rev. Lett.* **1996**, 76, 660.
- (37) Holm, B.; Ahuja, R. *J. Chem. Phys.* **1999**, 111, 2074.
- (38) Gibbs, G. V.; Rosso, K. M.; Teter, D. M.; Boysen, M. B., Jr.; Bukowinski, M. S. T. *J. Mol. Struct.* **1999**, 13, 485.